J. Appl. Comput. Mech., 12(1) (2026) 289-301
DOI: 10.22055/jacm.2025.48184.5040

ISSN: 2383-4536
jacm.scu.ac.ir

Shahid Chamran University of Ahvaz

Journal of Applied and Computational Mechanics

Research Paper

# Thermal Storage Improvement through the Melting Process of PCMs in Triplex Tube Heat Exchangers with Different Fin Materials

**Atef Chibani[1], Tawfiq Chekifi[2], Moustafa Boukraa[1]**

[1] Research Center in Industrial Technologies CRTI, P.O. Box 64, Cheraga 16014, Algiers, Algeria

[2] Unité de Recherche Appliqué en Energies Renouvelables, URAER, Centre de Développement des Energies Renouvelables, CDER, 47133, Ghardaïa, Algeria

Received January 26 2025; Revised May 29 2025; Accepted for publication June 02 2025.
✉ Corresponding author: T. CHEKIFI (t.chekifi@cder.dz)


**Abstract.** This study explores the melting dynamics of paraffin wax, a phase change material (PCM), within a Triplex Tube Heat Exchanger (THEX) equipped with internal fins, using numerical simulations. The primary objective is to evaluate the impact of fin materials—aluminum, copper, carbon, and steel—on the PCM melting rate under controlled conditions of 300 K ambient temperature and 373 K steam temperature. The results demonstrate that fins significantly enhance the melting rate by improving thermal conduction within the PCM. Aluminum, copper, and carbon fins exhibited superior performance, with aluminum fins achieving the greatest reduction in melting time, approximately 41% compared to the finless configuration. Steel fins, limited by lower thermal conductivity, reduced melting time by about 26%, reflecting a moderate improvement. Increasing the steam temperature to 383 K further accelerated melting across all cases, with the no-fin configuration showing a 10% reduction in melting time and finned configurations averaging a 5.3% reduction. These findings highlight the critical role of high-conductivity fin materials in optimizing thermal energy storage systems, particularly for thermal condenser applications, offering valuable insights for enhancing system efficiency.

**Keywords:** Melting process, Efficiency, Triplex tube heat exchanger, Phase change materials (PCM), Paraffin.

## 1. Introduction

Energy storage has consistently remained at the forefront of scientific inquiry, particularly in response to the challenges posed by fluctuating renewable energy sources [1]. Numerous innovative solutions have been proposed to efficiently capture and store excess energy. Among these, thermal energy storage (TES) is a highly promising approach, with systems leveraging sensible and latent heat, particularly through phase change materials (PCMs). PCMs are valued for their capacity to absorb and release significant heat during phase transitions. Consequently, the design and optimization of TES units have become central to research, advancing tank geometry, material integration, and thermal enhancement techniques [2]. TES systems incorporating PCMs have garnered significant interest due to their efficient energy storage and release capabilities [3], exceptional energy storage capabilities [4], and the near-constant temperature maintained during phase transitions [5]. Nonetheless, the primary drawback of latent heat storage is the notable issue of low thermal conductivity within PCMs and the resulting inefficiency in heat transfer within a TES system [6]. Consequently, there is a critical need to not only alter the characteristics of the PCMs but also to improve the heat transfer performance of the TES unit.

Numerous approaches to enhance the low thermal conductivity of PCMs have been explored [7-10]. These approaches include incorporating fins [11, 12], employing sinusoidal wall temperature or heat flux profiles [13-15], utilizing nanoparticles [16, 17], encapsulation techniques [18, 19], and integrating metal foam [20, 21]. Among these, fins are the most widely adopted due to their cost-effectiveness, efficiency, and ease of implementation [22]. As a result, both experimental and numerical investigations have extensively examined the effectiveness of fin-assisted TES systems. For instance, Sun et al. [23] tackled PCM's low thermal conductivity by introducing novel fin designs, such as arc-shaped and straight fins, to enhance heat transfer during charging and discharging. Compared to pure PCM systems, experimental results showed that these fins extended operating time during discharge by 54% to 90%. Numerical simulations indicated that arc and straight fins improved thermal performance by forming an effective thermal conduction network with longer fins and greater radial distance, extending working time by 157% at 20°C ambient temperature. Yan et al. [24] explored a dynamic ice-melting system using sprinkler nozzles to enhance discharge rates and temperature uniformity in ice-on-coil storage. Their experiments revealed a 60.7–89.2% increase in average discharge rate and a 45.3–54.3% reduction in melting time compared to static systems, with nozzle arrangement and flow parameters (e.g., brine temperature, flow rate) significantly affecting efficiency, particularly with staggered nozzles. Yan et al. [25] conducted experimental and numerical studies on heat transfer and energy storage in a double-layered enclosure filled with microencapsulated PCM (MEPCM). The enclosure, divided by an aluminum plate, was exposed to sinusoidal heat flux at the top and a constant low temperature at the bottom. Two paraffin-based MEPCMs with melting points of 28°C and 37°C were tested under varying heat fluxes (200–500 W/m²) and cold-wall temperatures (10–20°C). Gado [26] computationally analyzed Triply Periodic Minimal Surface (TPMS) structures (Gyroid, IWP, and Primitive) to improve charging performance in latent heat thermal energy storage (LHTES) systems, demonstrating that TPMS architectures enhance heat transfer through high surface-area-to-volume ratios and interconnected pore networks. Yan et al. [27] experimentally investigated ultrasonic-assisted dynamic ice melting in an ice storage system, finding that higher ultrasonic power (200–584 W) reduced melting time by 32–50% and increased cooling rates by 295% compared to static systems, while frequency (40–120 kHz) had minimal impact. Gado [28] developed PCM-integrated TPMS heat sinks (Gyroid, IWP, Primitive) for electronics cooling, achieving up to 26°C lower operating temperatures compared to pure PCM systems, with Gyroid structures performing best and higher TPMS density (10-30%) further enhancing thermal regulation. Wang et al. [29] improved heat exchanger performance using paraffin-core MEPCMs (28°C melting point) with expanded graphite (EG), achieving 132% higher thermal conductivity and 15°C better temperature control compared to pure MEPCM. Their copper/aluminum-finned system showed that 30% EG content optimally balanced conductivity improvement (294% faster heat transfer) with a 28% reduction in sensible heat capacity. Vahidhosseini et al. [30] compared 12 fin designs in PCM-filled triplex-tube heat exchangers, finding that 8 bidirectional tree-shaped fins (TSFs) outperformed anchor-shaped and radial fins, reducing melting/solidification times by 5.37%/11.75% through optimized heat-path distribution. The alternating inner ⇋ outer attachment strategy minimized thermal resistance pockets, maintaining uniform PCM temperature (±2°C variation). Wang et al. [31] investigated TES systems for managing heat in airborne equipment, focusing on the impact of high gravity intensities and directions on PCM melting in finned enclosures. Their results showed that fins reduced melting time by up to 46.0% compared to unfinned enclosures. Sharma et al. [32] examined the effect of a single fin's placement on confined PCM melting in a spherical TES unit using two-dimensional transient numerical simulations. A fixed-length fin positioned at different distances from the center in upward and downward directions increased total melting time by up to 72% when farther from the center, and by 63% and 47% in upward and downward directions, respectively. Fins are widely applied in TES systems, including heat exchangers (HEXs) [33, 34], electronics cooling [35, 36], solar collectors [37, 38], and building materials [39, 40]. Meanwhile, their most prominent and extensively utilized role is undoubtedly in the realm of HEXs. Luo et al. [41] studied PCM melting in HEXs with various combinations of bifurcation fractal fins. Their findings showed that combined fractal fin HEXs reduced PCM melting time by 68% compared to traditional fractal fin HEXs, with higher bifurcation levels and heat transfer areas initially decreasing melting time before stabilizing. Ao et al. [42] proposed a V-shaped fin design in a HEX-TES system, evaluating nineteen arrangements. Results showed that natural convection accelerated melting in the upper part of the unit, creating efficiency disparities between the upper and lower halves. Increasing fin number and length at the bottom improved performance, with optimized designs enhancing heat storage efficiency by 2.57 times and reducing TES time by 61.05%. Palmer et al. [43] developed a flow-dynamics-informed fin arrangement for triplex-tube HEXs to accelerate PCM melting. Numerical modeling identified optimal fin structures, achieving a 57.4% reduction in melting time, highlighting the critical role of fins in enhancing PCM melting efficiency while minimizing space usage.

Prior research on this topic has largely neglected systematic comparisons of how different fin materials impact PCM melting dynamics in triplex-tube heat exchangers (THEX), a configuration chosen for its effective balance of heat transfer efficiency (due to increased surface area) and compact design. Our study focuses on aluminum, copper, carbon, and steel fins, selected to represent: the highest practical thermal conductivities (aluminum, copper), emerging lightweight alternatives (carbon), and cost-effective industrial standards (steel). This selection allows for a direct assessment of how conductivity, mechanical durability, and economic considerations influence phase change performance in confined annular spaces. Although previous studies have extensively explored fin-enhanced PCM conductivity, significant gaps persist in understanding these material-specific effects:

- Material-specific performance comparisons in annular geometries,
- Quantitative analysis of how fin properties (conductivity, density) interact with triplex-tube hydrodynamics, and
- Practical insights for industrial thermal storage optimization.

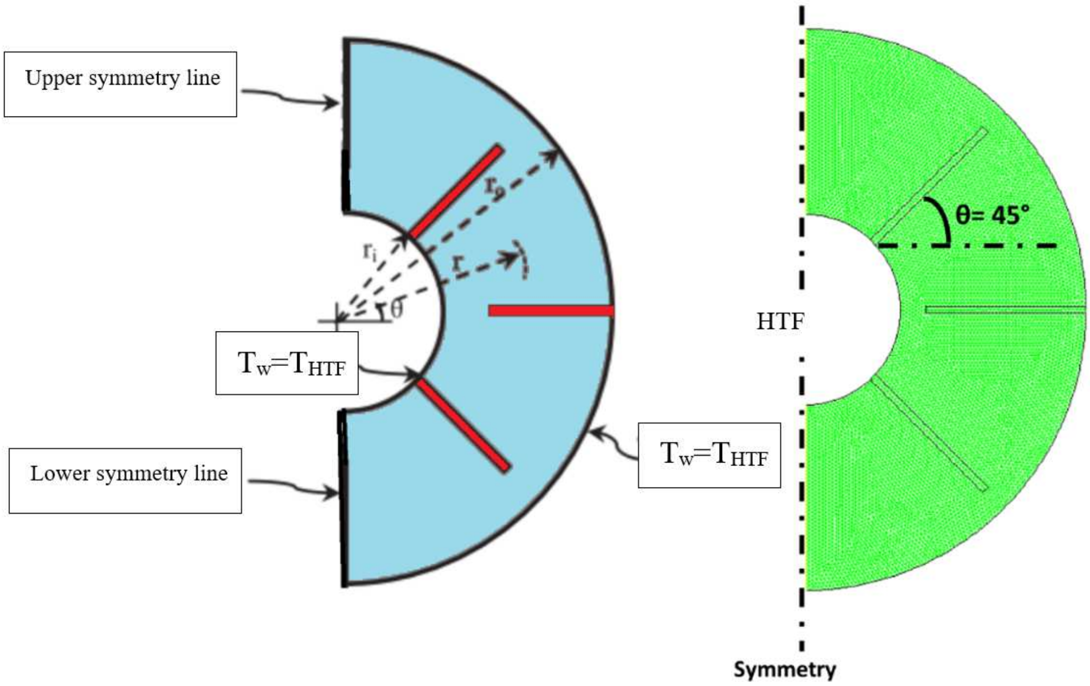


**Fig. 1.** Semi-transversal section of the triplex tube heat exchanger configuration.

This study fills critical knowledge gaps by employing a novel numerical approach to isolate the effects of fin materials under controlled conditions, providing actionable design insights. It focuses on the role of phase change materials (PCMs) in improving thermal performance, assessing their impact on heat storage and transfer efficiency. The triplex-tube system is rigorously evaluated as a benchmark configuration for advanced thermal storage applications, such as compact heat exchangers, solar energy systems, and thermal management of high-power electronics. By bridging fundamental material science with practical engineering design, this research makes significant contributions to both academic understanding and industrial innovation in PCM-based energy systems.

## 2. Mathematical Model and Numerical Method

The studied system is described in Fig. 1, the system consists of two circular rings with PCM material in the middle in a solid state. The walls of the two rings have fins and the whole are subjected to hot temperature.

Our configuration is composed of an annular structure with fins affixed to the inner surface, designed to enhance heat transfer and accelerate the melting process. The fins, made from various materials, are strategically positioned to maximize thermal conductivity. A cross-sectional view reveals this setup, while a top view provides a clear depiction of the fin arrangement within the unit. This research aims to optimize the design for efficient thermal energy storage by analyzing the impact of different fin materials on melting rates.

Based on the above assumptions, the conservation equations are presented as follows:

- **Momentum conservation equation**

$$\frac{\partial \rho}{\partial t}+\frac{\partial(\rho u)}{\partial x}+\frac{\partial(\rho v)}{\partial y}=0 \tag{1}$$

This equation is derived from Newton's second law applied to fluid motion along both the X and Y axes. The left-hand side represents total acceleration (both local and convective). On the right-hand side, the terms represent, respectively, the pressure gradient force, the viscous (diffusive) force.  The third term incorporates the Boussinesq approximation, capturing the influence of buoyancy-driven body forces due to gravity in the X and Y directions on the liquid paraffin.

The last term of Eqs. (2) and (3) was due to the mushy region during the phase change process.

- **Continuity equation:**

$$\frac{\partial(\rho u)}{\partial t}+u\frac{\partial(\rho u)}{\partial x}+v\frac{\partial(\rho u)}{\partial y}=-\frac{1}{\rho}\frac{\partial P}{\partial x}+\mu\left(\frac{\partial^2 u}{\partial x^2}+\frac{\partial^2 u}{\partial y^2}\right)+\rho g\beta_{\text{expansion}}\cos\beta\left(T-T_{ref}\right)+S_x \tag{2}$$

$$\frac{\partial(\rho v)}{\partial t}+u\frac{\partial(\rho v)}{\partial x}+v\frac{\partial(\rho v)}{\partial y}=-\frac{1}{\rho}\frac{\partial P}{\partial y}+\mu\left(\frac{\partial^2 v}{\partial x^2}+\frac{\partial^2 v}{\partial y^2}\right)+\rho g\beta_{\text{expansion}}\sin\beta\left(T-T_{ref}\right)+S_y \tag{3}$$

This equation expresses the conservation of mass within a fluid. The first term represents the local temporal change in density, while the second term denotes the mass flux due to fluid motion. $\rho$ represents the density. $u$ and $v$ denote the velocity in $x$ and $y$ directions, respectively. The left-hand side represents total acceleration (both local and convective). On the right-hand side, the terms represent, respectively, the pressure gradient force, the viscous (diffusive) force. $\beta_{\text{expansion}}$ represents the thermal expansion coefficient, $g$ represents gravitational acceleration of the PCM, $\theta$ represents the angle of incline of the collector, $T_{ref}$ represents the reference temperature, the terms $S_x$ and $S_y$ denote the source terms in the $x$- and $y$-directions, respectively [44], which originate from the mushy region formed during the phase change process.

The definitions of the source terms $S_x$ and $S_y$ are given as follows:

$$S_x=\frac{A_{mush}u(1-\gamma^2)}{(\gamma^3+\varepsilon)},\quad S_y=\frac{A_{mush}v(1-\gamma^2)}{(\gamma^3+\varepsilon)} \tag{4}$$

In this study, the symbol $\gamma$ represents the liquid fraction and $A_{mush}$ is a constant value specific to the mushy zone, equal to 105 $kgm^{-3}s^{-1}$. Additionally, a small value $\varepsilon$ is used to prevent division by zero, it is set to 0.001 [45, 46].

- **Energy equation:**

$$\frac{\partial(\rho H)}{\partial t}+u\frac{\partial(\rho H)}{\partial x}+v\frac{\partial(\rho H)}{\partial y}=k\left(\frac{\partial^2 T}{\partial x^2}+\frac{\partial^2 T}{\partial y^2}\right) \tag{5}$$

This equation reflects the conservation of thermal energy. The left-hand side includes heat accumulation and convective transport. The first term on the right-hand side describes heat conduction. The enthalpy ($H$) of the PCM can be expressed as the sum of the sensible enthalpy ($h$) and the latent heat enthalpy $(\Delta H)$ as follows [44, 47, 48]:

$$H=h+\Delta H \tag{6}$$

$$h=h_{ref}+\int_{T_{ref}}^{T}C_p dT \tag{7}$$

A grid independence study is essential in computational fluid dynamics (CFD) or any numerical simulation involving partial differential equations to ensure that the results are not significantly affected by the discretization of the domain.

The 12490 grids were chosen as the independent grid for the following reasons:

- Relative error less than 1% compared to the best grid.
- The convergence trend is clear and asymptotic.
- Computational time increases significantly beyond 12490, with a slight improvement in accuracy.

The enthalpy at the reference temperature $T_{ref}$ is represented by $h_{ref}$. The latent heat enthalpy $\Delta H$ can be determined by using the latent heat $L$ of the PCM through the following calculation [12, 49]:

$$\Delta H = \gamma L \tag{8}$$

The liquid fraction $\gamma$ is defined as follows [50]:

$$\gamma = \begin{cases} 0 & T < T_s \\ 1 & T > T_l \\ (T - T_s)/(T_l - T_s) & T_s < T < T_l \end{cases} \tag{9}$$

### 2.1. Initial and boundary conditions

The starting temperature of the simulated area was established as 27 °C, at which point the PCM is fully solid:

$$T_{int} = 27C^\circ \text{ , } T_{HTF} = 100C^\circ \tag{10}$$

The boundary conditions of the TTHX were varied for the PCM freezing types used, and for the other different cases, and can be written as below.

The inside freezing methods:

$$r = r_i \text{ , } T_{HTF} = 100C^\circ \tag{11}$$

$$r = r_m \text{ , } \frac{\partial H}{\partial r} = 0 \tag{12}$$

The outside freezing methods:

$$r = r_m \text{ , } T_{HTF} = 100C^\circ \tag{13}$$

$$r = r_i \text{ , } \frac{\partial H}{\partial r} = 0 \tag{14}$$

Both tubes method and other cases:

$$r = r_i \text{ , } T_{HTF} = 100C^\circ \tag{15}$$

$$r = r_m \text{ , } T_{HTF} = 100C^\circ \tag{16}$$

The initial temperature for all cases is:

$$t = 0, T_{TTHX} = 27C^\circ \tag{17}$$

## 3. Numerical Procedure and Validation

### 3.1. Simulation parameters

The Ansys fluent 15.0 commercial CFD software was used to find the numerical solution. The energy and momentum equations were solved using a second-order up-winding scheme, and the PRESTO Scheme was used for the pressure [44, 45, 51]. The PISO was employed to handle the coupling between velocity and pressure [52]. To improve the stability during the convergence, the under-relaxation factors for momentum, pressure, liquid fraction, and energy were set to 0.7, 0.3, 0.9, and 1, respectively [53]. The maximum number of iterations for each time step was set to 100, which met the convergence criteria for energy and velocity of $10^{-7}$ and $10^{-5}$, respectively.

### 3.2. Time step and grid size independency tests

An exploration into the optimal mesh cell count was conducted, considering various cell numbers (12490, 14773 and 17483) with a time step of 0.1 second, as illustrated in Fig. 2.

The results clearly reveal that, for the current model, a mesh with 14773 cells has the best efficiency and shows the least amount of divergence even when the number of cells is increased to 17483. This careful selection accomplishes two goals at once: accurate representation and computational efficiency. Applying this study to the whole range of applicable heat exchanger types, a mesh arrangement consisting of 14773 cells was selected. Moreover, the choice of an ideal time step was shown to be an important aspect. After careful investigation with time step sizes of 0.25, 0.1, and 0.075 seconds on a mesh of 14773 cells, as shown in Fig. 2(a), the ultimate decision indicates that a 0.1s time step is the best option. This choice, which is based on a thorough evaluation, guarantees that temporal dynamics and the spatial complexities captured by the selected mesh arrangement are in harmony.

**Table 1.** Thermo-physical properties of chosen materials as PCM measured at 25°C [54, 55].

| Material | $\rho$ (kg/m$^3$) | λ (W/m.K) | $C_p$ (J/kg.K) | Latent heat (J/kg) | Phase change temperature (°C) |
|---|---|---|---|---|---|
| Paraffin wax (RT70HC) | 880/770 | 0.2 | 2000 | 260000 | 69-71 |
| Graphite | 2266 | 170 | 720 | - | - |
| Aluminum | 4850 | 202.4 | 871 | - | - |
| Steel | 7830 | 13 | 468 | - | - |
| Copper | 8933 | 350-401 | 381 | - | - |

### 3.3. Model validation

This section also contains the results of validation test. This study is based on repeating previous experiments and comparing their results with the results of our new method.

The thermo-physical properties of the materials used as fins in the study, as detailed in Table 1, highlight significant differences in their ability to conduct heat and store thermal energy. Paraffin wax (RT70HC) serves as the phase change material (PCM) with a density of 880/770 kg/m³, a low thermal conductivity of 0.2 W/m·K, a high specific heat capacity of 2000 J/kg·K, and a latent heat of 260000 J/kg, transitioning between 69-71°C.

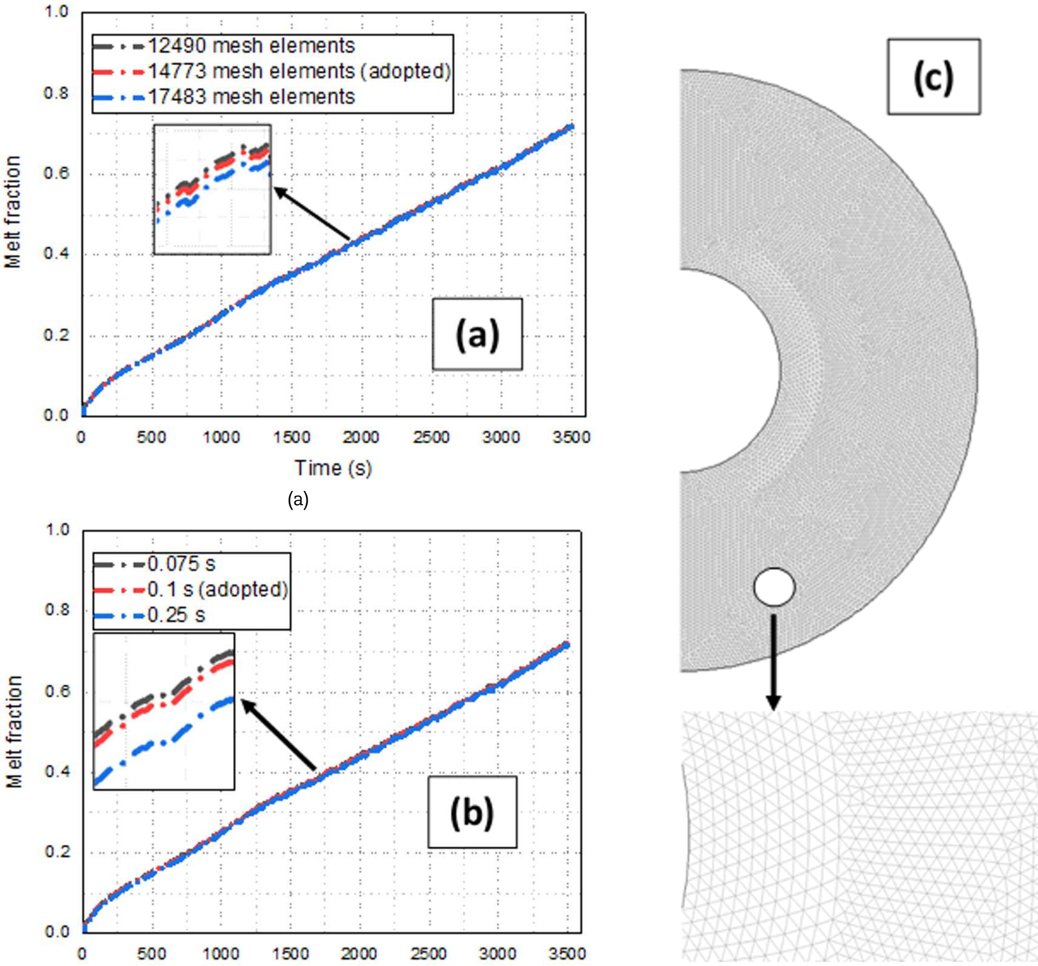


(a) (b) (c)

**Fig. 2.** (a) Grid size, (b) time-step dependence of the numerical solution, (c) mesh type.

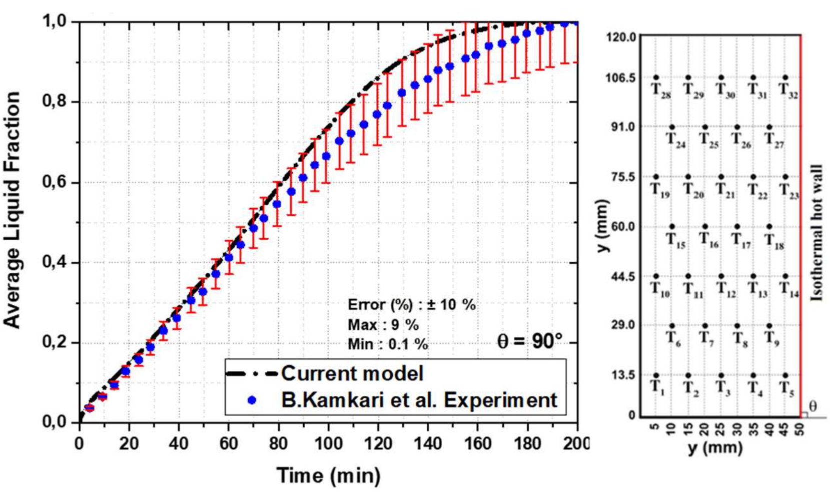


(a)

**Fig. 3.** Validation of the present model against (a) Kamkari et al.'s [56] experimental data, and (b) the numerical model by Al-Abidi et al. [50], showing good agreement.

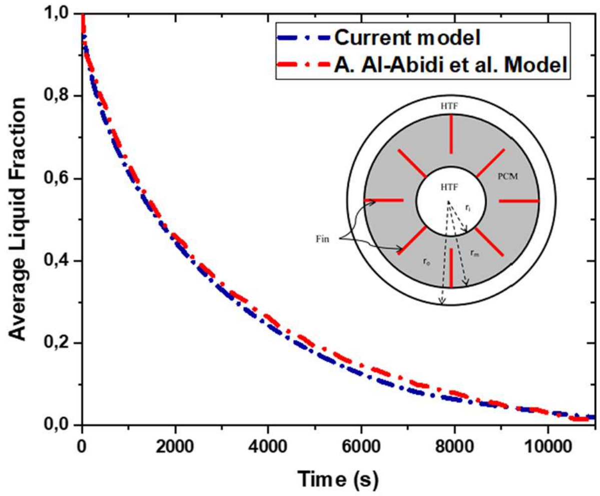


(b)

**Fig. 3.** Continued.

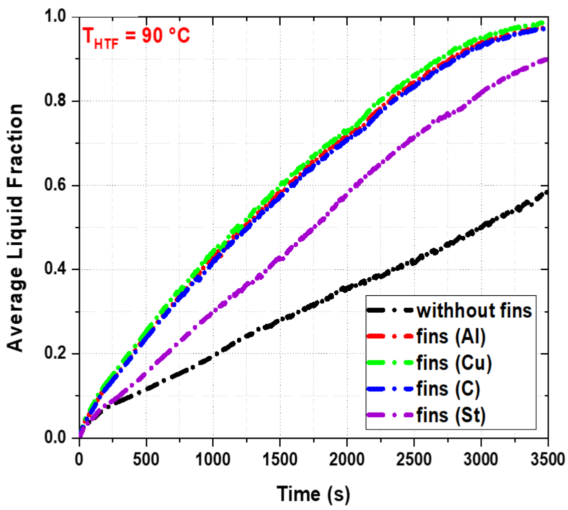


(a)

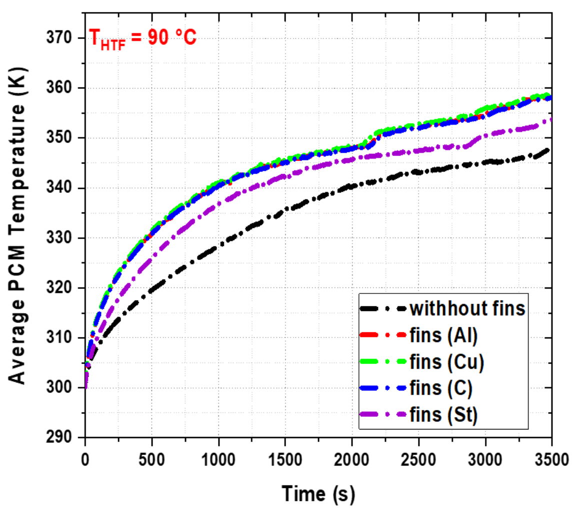


(b)

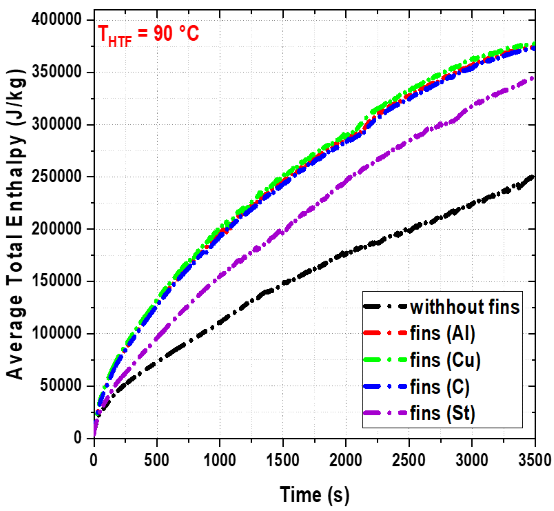


(c)

**Fig. 4.** Comparison of the liquid fractions, temperature and total enthalpy of finned and unfinned tube for $T_{HTF}$ = 90 °C.

The fin materials exhibit varied properties: graphite has an excellent thermal conductivity of 170 W/m·K, aluminum and copper offer even higher conductivities at 202.4 and 350-401 W/m·K, respectively, while steel, though dense at 7830 kg/m³, has a relatively low conductivity of 13 W/m·K. These differences in thermal properties are crucial in influencing the rate of heat transfer and the overall efficiency of the melting process within the triplex tube heat exchanger.

Figure 3 presents a comprehensive validation of the current numerical model against both experimental and numerical reference studies. In Fig. 3(a), the average liquid fraction during the melting process is compared with the experimental data of Kamkari et al. [56], showing a strong agreement. The maximum deviation between the current model and the experiment is 5.28%, while the average error is 4.84%, confirming the model's robustness in capturing melting dynamics. In Fig. 3(b), the solidification process is evaluated against the numerical model of Al-Abidi et al. [50], revealing highly consistent results with a maximum error of only 0.5% and an average error of 0.38%. The top right image displays the arrangement of temperature sensors in the experimental setup, and the bottom right diagram illustrates the computational domain used for simulations. Overall, these comparisons demonstrate the model's high accuracy and reliability in predicting both melting and solidification behavior of PCMs, supporting its suitability for thermal energy storage applications.

## 4. Results and Discussion

### 4.1. Heat and mass transfer

This study investigates the heat transfer and melting dynamics of paraffin in a horizontally oriented annular medium. To enhance the melting process, fins were incorporated on the inner walls of the system. The research specifically examines how the melting rate of the PCM (phase change material) is influenced by the type of fin material. Four materials were evaluated: aluminum, copper, steel, and graphite. The melting of a solid PCM evolves dynamically over time. To frame our findings, we first describe the key physical mechanisms governing phase-change heat transfer. When a PCM is heated, it absorbs thermal energy, triggering both conduction and buoyancy-driven convection. As melting begins, the lower-density liquid phase forms, generating density gradients that drive natural convection currents. This coupled heat and mass transfer significantly accelerates melting compared to conduction alone. Conversely, in the solid phase, denser hot spots collapse downward due to gravity, a process known as free convection. In the liquid phase, heat transfer occurs without material movement, referred to as conduction mode. Additionally, PCMs are characterized by their ability to transition between physical states under the influence of temperature (thermal energy), with each material having a specific temperature that dictates its phase. The thermal properties of the materials used in this study are presented in Table 1.

The study initially observes a progressive increase in the liquid fraction over time, particularly near the heated walls, confirming the gradual transition of the PCM from solid to liquid as it absorbs heat from high-temperature surfaces (Figs. 4 and 5). The inclusion of fins significantly enhances this process by expanding the effective heat transfer surface area, thereby accelerating thermal conduction into the PCM. In the absence of fins, the liquid fraction remains relatively low, reaching a maximum of approximately 0.68 at a heat transfer fluid temperature (THTF) of 90°C after 3500 s, indicating a slower melting rate.

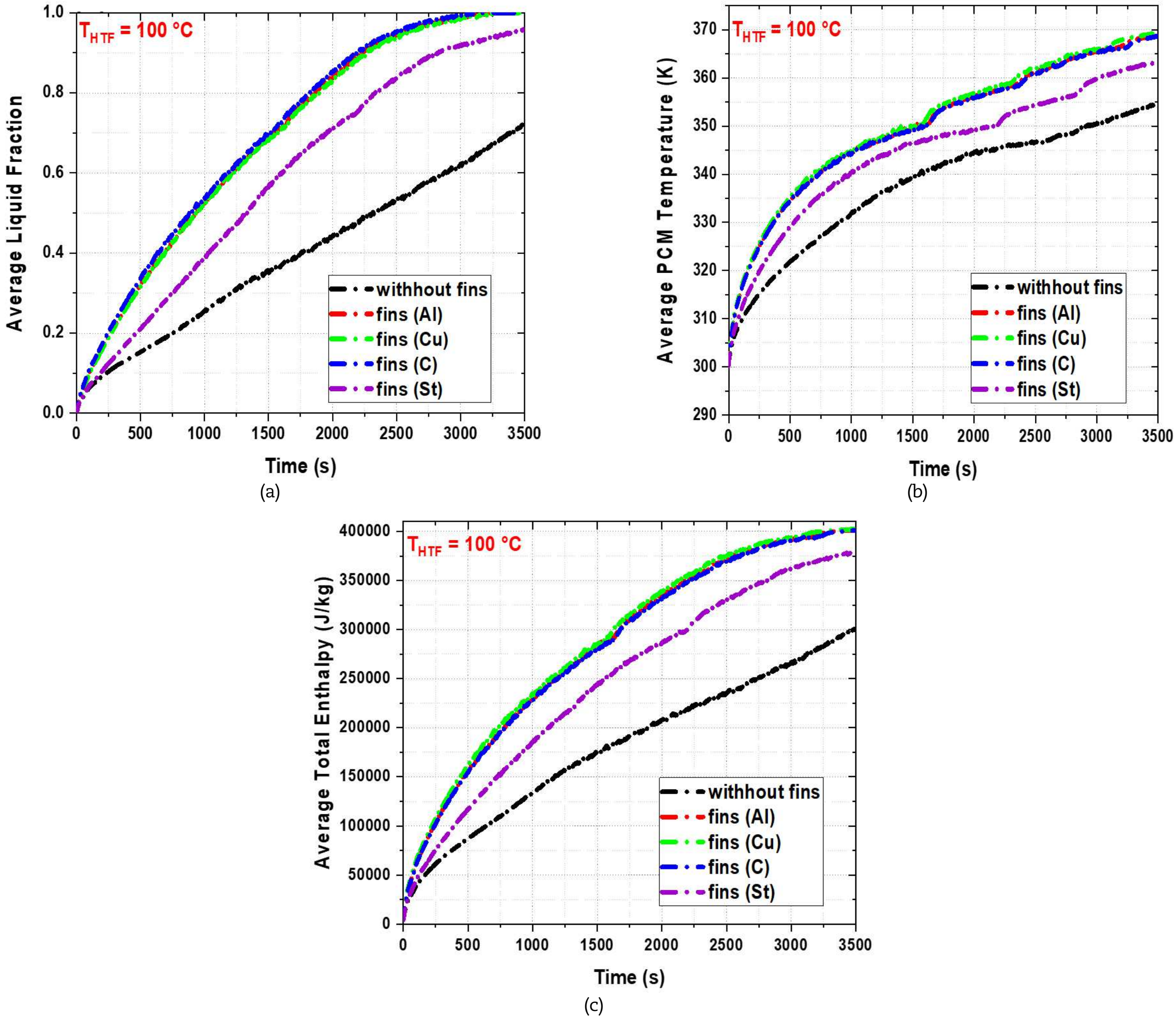


**Fig. 5.** Comparison of the liquid fractions, temperature and total enthalpy of finned tube for $T_{HTF}$ = 100 °C.

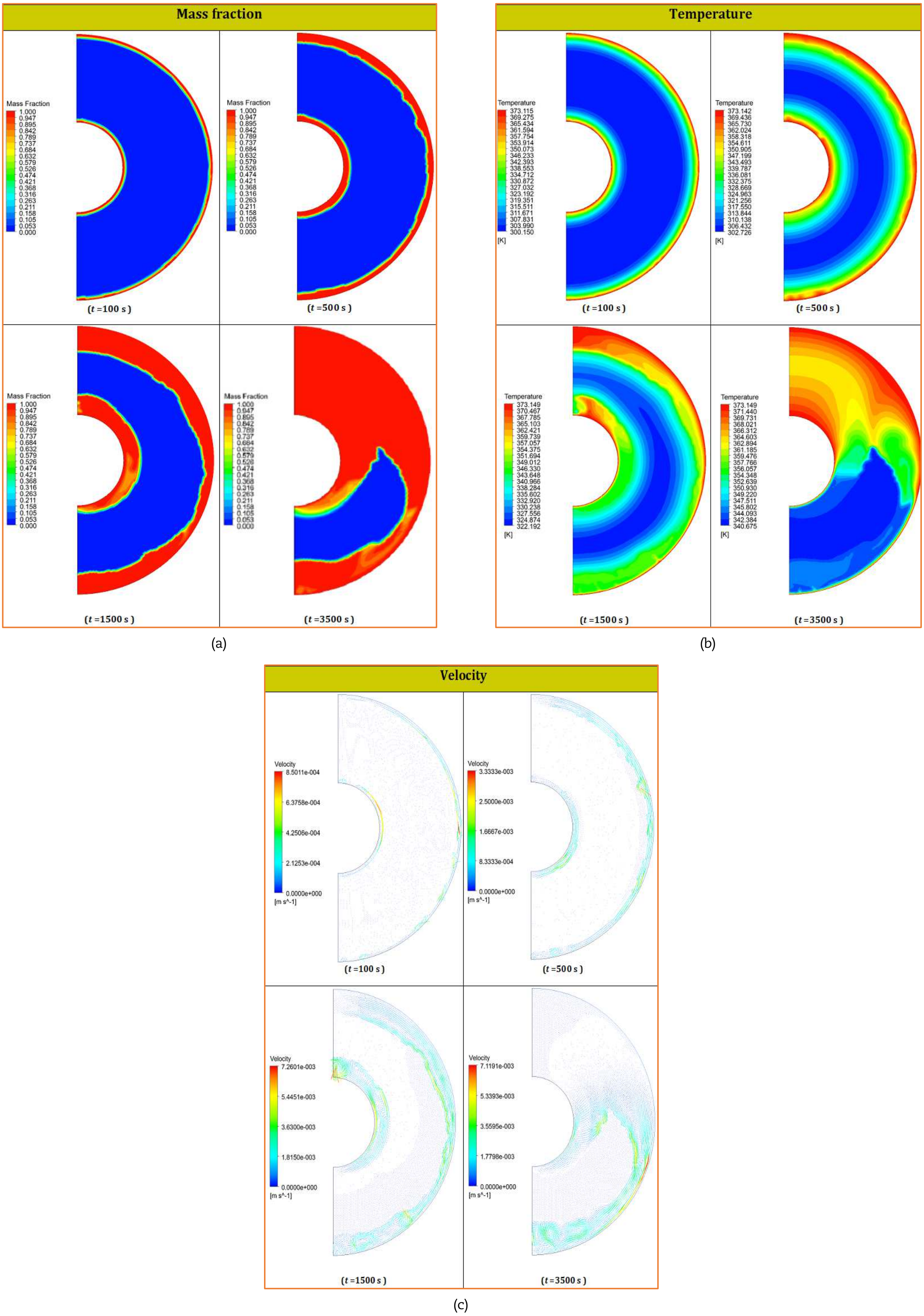


**Fig. 6.** Distributions of the (a) liquid fraction, (b) temperature and (c) velocity for the computational domains of the PCM without fins for $t$ = 100 s, $t$ = 50 s, $t$ = 1500 s, $t$ = 3500 s.

In contrast, systems with aluminum, copper, and carbon fins achieve complete melting in approximately 3200 s, demonstrating their superior thermal performance. Steel fins, with a lower thermal conductivity (~50 W/m·K), result in slower melting, achieving full melting only after about 3400 s. This trend is reflected in the average PCM temperature evolution. Without fins, the temperature rises more gradually, reaching approximately 352 K by the end of the simulation at 90°C. Steel fins provide a moderate improvement, while aluminum, copper, and carbon fins elevate the PCM temperature to around 367 K, indicating faster heat penetration and a more efficient phase transition. Similarly, the total enthalpy evolution underscores the energy storage capacity for each configuration. At THTF = 90°C, systems with aluminum, copper, or carbon fins achieve enthalpy values of approximately 385,000 J/kg, compared to only about 290,000 J/kg for the no-fin case. Steel fins yield intermediate results. This comparative analysis highlights the pivotal role of fin material in optimizing heat transfer and accelerating the melting process. Aluminum, copper, and carbon fins consistently outperform, while steel provides moderate improvements. These findings remain consistent across both tested heat transfer fluid temperatures (90°C and 100°C), confirming the reliability of the simulation and emphasizing the value of high-conductivity materials in enhancing the efficiency of latent heat thermal storage.

Figure 6 depicts the mass fraction, temperature distribution, and velocity streamlines at 100, 500, 1500, and 3500 seconds for configurations without fins, providing insight into the phase-change material (PCM) melting process. At the initial stage (100 seconds), melting is concentrated near the walls, where the material appears dense and red, indicating peak melting with temperatures between 350 K and 373 K, corresponding to a fully liquefied state. Blue regions represent solid paraffin below its melting point, a consequence of its low thermal conductivity. By 1500 seconds, melting remains relatively uniform, with a higher concentration of molten material near the walls, where liquid velocity reaches approximately 0.007 m/s before gradually decreasing to zero, leaving some material solid. Gravity's influence becomes evident by 3500 seconds, with buoyancy effects causing irregular melting patterns. The upper half of the domain shows increased molten PCM density, driven by natural convection currents that enhance phase change. Temperature distribution becomes uneven, with the upper region reaching ~373 K, while the lower, solid-dominated region remains below 340 K. Fluid velocity within the reactor core increases due to intensified buoyant forces. In contrast, Fig. 6 also analyzes the finned configuration, revealing distinct fluid fraction and temperature evolution within the heat exchanger. The presence of fins results in a significantly faster and more uniform melting process compared to the finless case, primarily due to increased surface area and enhanced thermal conductivity. At 1500 seconds, fins that rapidly heat up facilitate more effective heat transfer, though thermal conductivity is not the only factor. The density and specific heat capacity of the fin material also play critical roles. While metals may exhibit similar thermal conductivities, cost-effectiveness varies. For instance, copper fins demonstrated superior thermal performance at 1500 seconds, with the liquid phase forming and dispersing evenly, driven by enhanced heat transfer into the paraffin via the fins and hot boundary walls. However, the upper fins' temperature does not always immediately match the heating fluid's temperature, due to the metal's physical properties affecting heat absorption and conduction rates. Fins enhance both thermal conduction and natural convection in the PCM. In the liquid phase, paraffin achieves a velocity of ~0.005 m/s. Notably, in finned configurations, buoyant forces have a reduced impact, as molten material distributes more uniformly across fin surfaces. This suggests that fins significantly improve heat transfer efficiency and reduce overall melting time. Without fins, the liquid phase acts as a barrier, slowing heat transfer to the remaining solid PCM, underscoring the importance of thermal conductivity. Additionally, alternatives like metallic foams or nanoparticles could further enhance the system's heat transfer performance.

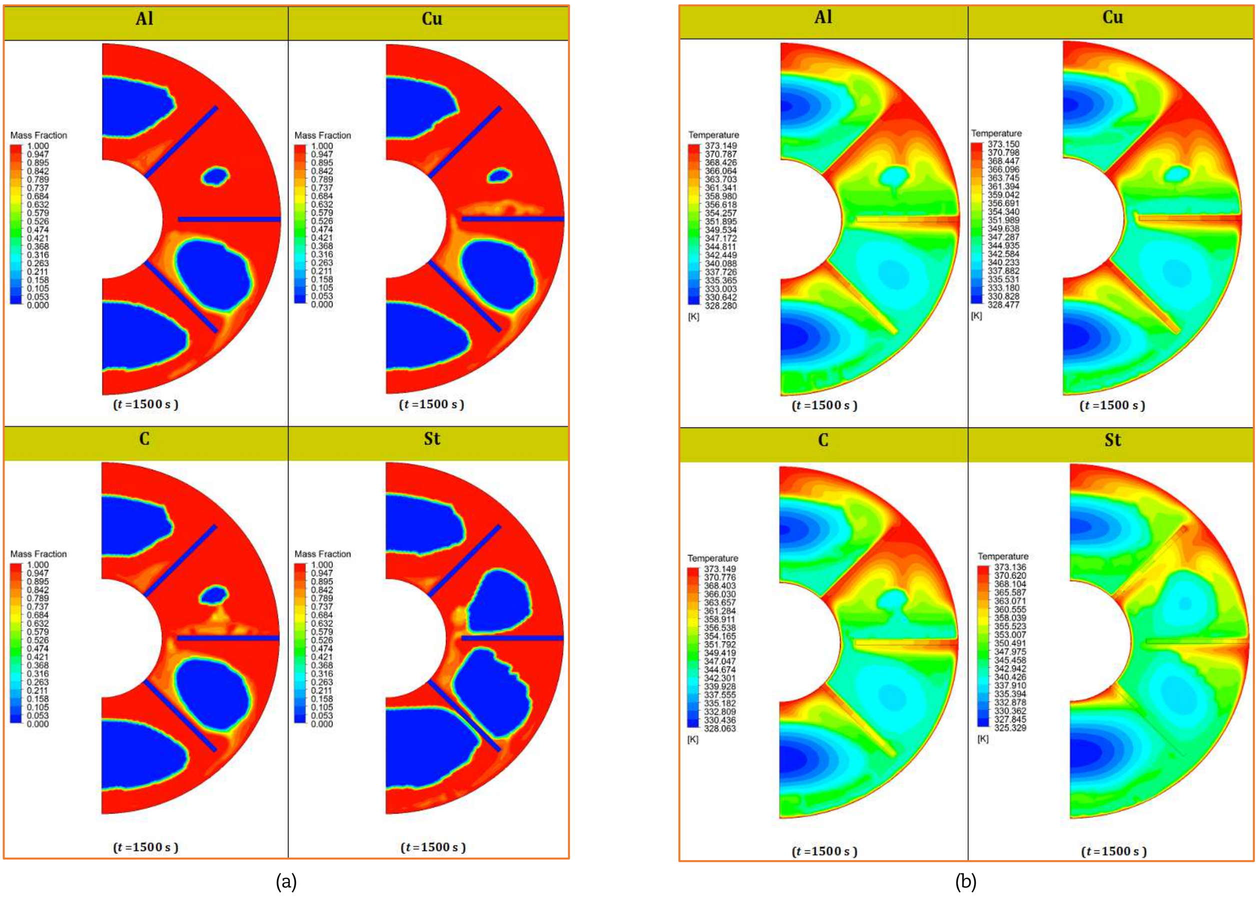


**Fig. 7.** Distributions of the (a) liquid fraction, (b) temperature and (c) velocity for the computational domains of the PCM with fins for $t$ = 1500 s.

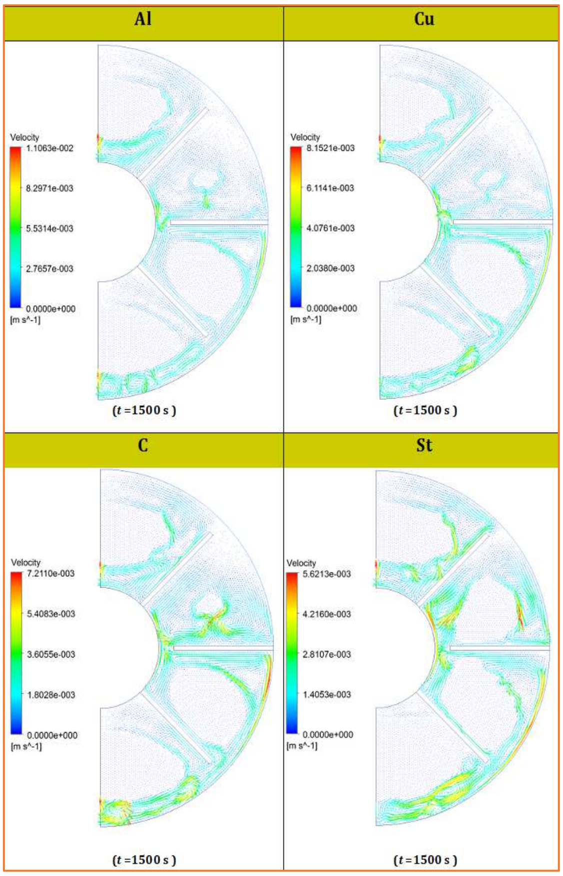


(c)

**Fig. 7.** Continued.

Figure 7 illustrates the liquid fraction distributions within the PCM at $t$ = 1500 s for different fin materials: carbon, aluminum, copper, and steel, revealing distinct melting patterns. Aluminum fins produce a significantly larger molten region, reflecting enhanced heat transfer and accelerated PCM melting, likely due to aluminum's high thermal conductivity (202.4 W/m·K), which facilitates efficient heat dissipation into the PCM. In contrast, copper, carbon, and steel fins exhibit progressively smaller molten areas, indicating slower melting rates. Despite copper's strong thermal conductivity (350-401 W/m·K), its performance appears limited by factors such as fin geometry or interfacial contact resistance. Carbon and steel, with lower thermal conductivities (5–50 W/m·K), show even more constrained melting zones. These results highlight the critical influence of fin material on optimizing PCM melting. However, a deeper analysis incorporating temperature and velocity distributions over time is needed to fully understand the underlying mechanisms and quantify performance differences among the materials.

Figure 7(b) presents detailed temperature profiles within the PCM at $t$ = 1500 s for aluminum, copper, carbon, and steel fins, revealing distinct thermal behaviors. Aluminum fins achieve a relatively uniform temperature distribution, indicative of efficient heat conduction and dissipation, which aligns with their observed rapid melting rate. This homogeneity reflects optimal heat transfer from the fins to the PCM. Copper fins, despite their high thermal conductivity, display a noticeable temperature gradient, with higher temperatures near the fins suggesting impeded heat transfer, possibly due to interfacial thermal resistance. This contributes to copper's slower melting rate. Carbon and steel fins, with their lower thermal conductivities, exhibit even steeper temperature gradients, with elevated temperatures concentrated near the fins, indicating significant thermal resistance that limits heat transfer to the PCM and results in the slowest melting rates. The temperature contours in Fig. 7(b) underscore the pivotal role of fin material in the thermal performance of PCM systems. Aluminum emerges as the optimal material, leveraging its high conductivity to achieve uniform temperature distribution and accelerate melting by 28.4% compared to unfinned cases. Carbon and steel, constrained by lower conductivities, generate localized thermal gradients that hinder heat transfer and prolong melting times. Copper shows intermediate performance, suggesting that optimizing fin geometry or improving interfacial contact could enhance its effectiveness. These findings offer valuable guidance for designing high-efficiency thermal storage systems.

Figure 7(c) provides velocity vectors that reveal fluid flow patterns within the PCM. Aluminum fins generate a robust and organized velocity field with distinct recirculation zones, promoting effective fluid mixing and circulation critical for efficient heat transfer throughout the PCM. In contrast, copper fins exhibit a less pronounced velocity field with weaker recirculation, indicating reduced fluid mixing compared to aluminum. Carbon and steel fins show even weaker velocity fields with minimal recirculation, suggesting limited fluid motion that hampers heat transfer and slows the melting process. The velocity profiles in Fig. 7(c) align closely with the thermal performance observed in Fig. 7(b). The strong velocity field of aluminum fins supports their uniform temperature distribution and accelerated melting rate, while the weaker fields of copper, carbon, and steel fins correspond to less efficient heat transfer and slower melting. These results emphasize the critical role of fluid dynamics in enhancing heat transfer and melting in PCM systems, with aluminum fins offering significant advantages due to their ability to induce robust fluid motion.

### 4.2. Melting time

Figure 8 presents the total melting time for tow value of temperature and several fins material, providing insight into the influence of both parameters on the melting behavior of PCM. in both cases ($T$ = 90°C and 100°C), the melting time is highest for without fins case, followed by stainless steel fins, followed by elites in copper, aluminum and carbon as presented in Fig. 8.

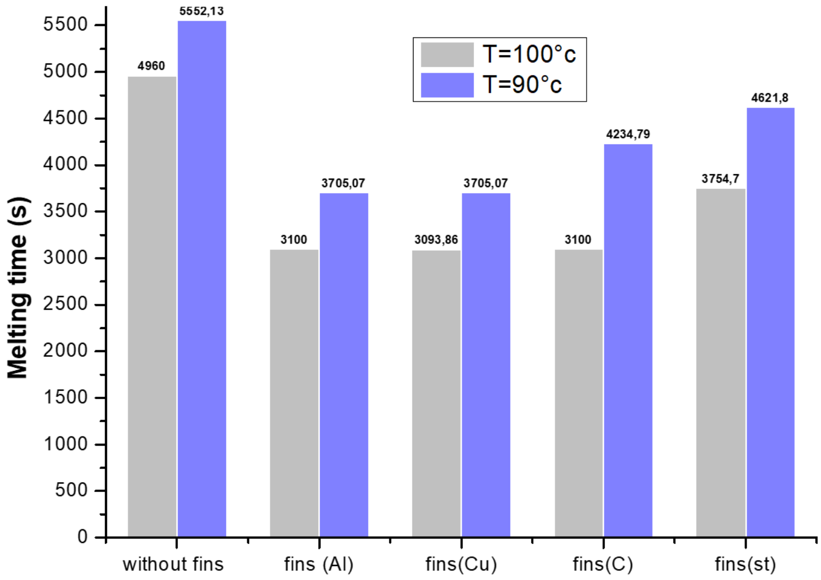


**Fig. 8.** Effect of different fin materials (Al, Cu, C, and ST) on the melting time of PCM in a triplex tube heat exchanger under two boundary temperatures (90°C and 100°C).

Figure 8 provides a comparative analysis of PCM melting times at two heating temperatures (90°C and 100°C) across various fin configurations. The data clearly demonstrate that fins significantly enhance melting performance by reducing total melting time compared to the baseline case without fins. At 90°C, the finless configuration exhibited the longest melting time of 5552.13 s. Incorporating aluminum and copper fins reduced this to 3705.07 s, a 33.27% improvement over the finless case. Carbon fins achieved a moderate reduction to 4234.79 s (23.73% improvement), while stainless steel fins lowered the melting time to 4621.8 s, a 16.76% enhancement. At 100°C, melting times decreased across all configurations due to the higher boundary temperature. The finless setup improved to 4960 s, a 12% reduction. Copper fins recorded the fastest melting time at 3093.86 s, closely followed by aluminum and carbon fins at approximately 3100 s each, reflecting reductions of 37.5–37.6% compared to the finless baseline. Stainless steel fins achieved a 24.3% reduction, with a melting time of 3754.7 s. These results highlight two key insights: (1) the thermal conductivity of fin materials significantly impacts melting rates, with copper and aluminum outperforming others due to their superior heat conduction, and (2) while higher heating temperatures enhance melting efficiency across all configurations, the use of high-conductivity fins provides a more substantial improvement than temperature increases alone.

## 5. Conclusion

This study examined the melting behavior of a phase change material (PCM) within a toroidal space fitted with fins on its inner surfaces, focusing on the impact of fin material and presence on the melting process. The key findings are as follows:

- Fins significantly accelerate the melting process compared to a finless configuration by enhancing heat transfer.
- The choice of fin material plays a critical role in determining the melting rate, with aluminum, copper, and carbon fins outperforming steel.
- Aluminum fins exhibited the best performance, driven not only by their high thermal conductivity but also by their ability to induce stronger natural convection in the molten PCM. This led to a more uniform temperature distribution and improved heat transfer, achieving complete melting in approximately 1320 seconds, compared to over 2200 seconds for the no-fin case.
- Temperature contour analysis confirmed that aluminum fins promoted a more uniform heat distribution across the PCM, minimizing thermal gradients.
- Velocity vector plots indicated enhanced fluid circulation near the fin surfaces in the aluminum configuration, further facilitating efficient energy absorption and phase transition.
- Steel fins, limited by their lower thermal conductivity, showed a modest performance improvement, reducing melting time by approximately 26%, with sharper temperature gradients and weaker induced flow.
- Copper and carbon fins also performed effectively, with melting times within 4% of aluminum fins, highlighting their comparable thermal behavior under the tested conditions.

These results underscore the potential of fin-enhanced PCM systems for thermal energy storage applications. Further research is needed to optimize fin geometry, spacing, and material selection tailored to specific operating conditions and PCM properties.

## Author Contributions

A. Chebani planned the scheme, conducted simulation and initiated the project; M. Boukraa and T. Chekifi developed the mathematical modeling and examined the theory validation. The manuscript was written through the contribution of all authors. All authors discussed the results, reviewed, and approved the final version of the manuscript.

## Acknowledgments

The authors sincerely thank all individuals who contributed to the successful completion of this work. Special appreciation is extended to those who provided technical support, offered insightful feedback, and rendered valuable assistance during the experimental phase and data analysis.

## Conflict of Interest

The authors declared no potential conflicts of interest concerning the research, authorship, and publication of this article.

## Funding

The authors received no financial support for the research, authorship, and publication of this article.

## Data Availability Statements

The datasets generated and/or analyzed during the current study are available from the corresponding author on reasonable request.

## References

[1] Chekifi, T., Boukraa, M., CFD applications for sensible heat storage: A comprehensive review of numerical studies, *Journal of Energy Storage*, 68, 2023, 107893.
[2] Chekifi, T., Boukraa, M., Thermocline storage for concentrated solar power plants: Descriptive review and critical analysis, *Journal of Energy Storage*, 55, 2022, 105773.
[3] Yang, Y., Pang, Y., Liu, Y., Guo, H., Preparation and thermal properties of polyethylene glycol/expanded graphite as novel form-stable phase change material for indoor energy saving, *Materials Letters*, 216, 2018, 220-223.
[4] Rahmalina, D., Rahman, R. A., Increasing the rating performance of paraffin up to 5000 cycles for active latent heat storage by adding high-density polyethylene to form shape-stabilized phase change material, *Journal of Energy Storage*, 46, 2022, 103762.
[5] Du, K., Calautit, J., Wang, Z., Wu, Y., Liu, H., A review of the applications of phase change materials in cooling, heating and power generation in different temperature ranges, *Applied Energy*, 220, 2018, 242-273.
[6] Khademi, A., et al., A brief review on different hybrid methods of enhancement within latent heat storage systems, *Journal of Energy Storage*, 54, 2022, 105362.
[7] Sun, X., et al., Investigation of heat transfer enhancement in a triple TUBE latent heat storage system using circular fins with inline and staggered arrangements, *Nanomaterials*, 11, 2021, 2647.
[8] Surya, A., Prakash, R., Nallusamy, N., Heat transfer enhancement and performance study on latent heat thermal energy storage system using different configurations of spherical PCM balls, *Journal of Energy Storage*, 72, 2023, 108643.
[9] Hu, Z., et al., Numerical investigation of the melting characteristics of spherical-encapsulated phase change materials with composite metal fins, *Journal of Energy Storage*, 68, 2023, 107902.
[10] Khan, J., Kaur, I., Aider, Y., Cho, H., Choi, S., Singh, P., Transient thermal performance enhancement of phase change material (RT82) through novel pin arrangements under varied gravity conditions, *Numerical Heat Transfer, Part A: Applications*, 85, 2024, 1157-1171.
[11] Mozafari, M., Hooman, K., Lee, A., Cheng, S., Numerical study of a dual-PCM thermal energy storage unit with an optimized low-volume fin structure, *Applied Thermal Engineering*, 215, 2022, 119026.
[12] Mahdi, J. M., Nsofor, E. C., Solidification enhancement of PCM in a triplex-tube thermal energy storage system with nanoparticles and fins, *Applied Energy*, 211, 2018, 975-986.
[13] Bouzennada, T., Mechighel, F., Filali, A., Kolsi, L., Study of the usability of sinusoidal function heat flux based on enthalpy-porosity technique for PCM-related applications, *Journal of Thermal Analysis and Calorimetry*, 141, 2020, 1769-1784.
[14] Mehrjardi, S. A. A., Khademi, A., Ushak, S., Alotaibi, S., Melting process of various phase change materials in presence of auxiliary fluid with sinusoidal wall temperature, *Journal of Energy Storage*, 52, 2022, 104779.
[15] Chekifi, T., Boukraa, M., Thermo-hydraulic performance improvement of curved tube receiver operating without and with nanofluid, *Journal of Thermal Analysis and Calorimetry*, 148, 2023, 9183-9196.
[16] Chibani, A., Merouani, S., Bougriou, C., Dehane, A., Heat and mass transfer characteristics of charging in a metal hydride-phase change material reactor with nano oxide additives: the large scale-approach, *Applied Thermal Engineering*, 213, 2022, 118622.
[17] Wu, Y., et al., Synergistic enhancement of heat transfer and thermal storage characteristics of shell and tube heat exchanger with hybrid nanoparticles for solar energy utilization, *Journal of Cleaner Production*, 387, 2023, 135882.
[18] Tat, S. A., Muthukumar, P., Mondal, P. K., Design, development and performance investigations of a latent heat storage with PCM encapsulation, *Journal of Energy Storage*, 72, 2023, 108695.
[19] Selimefendigil, F., Öztop, H. F., Multijet impingement heat transfer under the combined effects of encapsulated-PCM and inclined magnetic field during nanoliquid convection, *International Journal of Heat and Mass Transfer*, 203, 2023, 123764.
[20] Chibani, A., Merouani, S., Benmoussa, F., Computational analysis of the melting process of Phase change material-metal foam-based latent thermal energy storage unit: The heat exchanger configuration, *Journal of Energy Storage*, 42, 2021, 103071.
[21] Shu, G., Xiao, T., Guo, J., Wei, P., Yang, X., He, Y.-L., Effect of charging/discharging temperatures upon melting and solidification of PCM-metal foam composite in a heat storage tube, *International Journal of Heat and Mass Transfer*, 201, 2023, 123555.
[22] Shahsavar, A., Goodarzi, A., Mohammed, H. I., Shirneshan, A., Talebizadehsardari, P., Thermal performance evaluation of non-uniform fin array in a finned double-pipe latent heat storage system, *Energy*, 193, 2020, 116800.
[23] Sun, Z., Fan, R., Zheng, N., Thermal management of a simulated battery with the compound use of phase change material and fins: Experimental and numerical investigations, *International Journal of Thermal Sciences*, 165, 2021, 106945.
[24] Yan, W.-M., Gao, K.-E., Sajjad, U., Chien, L.-H., Amani, M., Experimental study of dynamic melting process in an ice-on-coil storage system, *Journal of Energy Storage*, 73, 2023, 109177.
[25] Yan, W.-M., Lin, Y.-F., Sajjad, U., Yang, T.-F., Rashidi, S., Experimental and numerical study on heat transfer and energy storage characteristics in double-layered enclosure packed with microencapsulated phase change material, *International Journal of Heat and Fluid Flow*, 112, 2025, 109757.
[26] Gado, M. G., Improving the charging performance of latent heat thermal energy storage systems using triply periodic minimal surface (TPMS) structures, *Journal of Energy Storage*, 103, 2024, 114310.
[27] Yan, W.-M., Yeh, R.-S., Sajjad, U., Chien, L.-H., Amani, M., Performance evaluation of ultrasonic-assisted dynamic ice melting in ice storage systems: An experimental study, *Journal of Energy Storage*, 103, 2024, 114045.
[28] Gado, M. G., Thermal management and heat transfer enhancement of electronic devices using integrative phase change material (PCM) and triply periodic minimal surface (TPMS) heat sinks, *Applied Thermal Engineering*, 258, 2025, 124504.
[29] Wang, T.-H., Yang, T.-F., Kao, C.-H., Yan, W.-M., Ghalambaz, M., Paraffin core-polymer shell micro-encapsulated phase change materials and expanded graphite particles as an enhanced energy storage medium in heat exchangers, *Advanced Powder Technology*, 31, 2020, 2421-2429.
[30] Vahidhosseini, S. M., Esmaeili, Z., Rashidi, S., Rafee, R., Yan, W.-M., Effects of novel fins on PCM melting/solidification in triplex tube heat exchangers, *Applied Thermal Engineering*, 262, 2025, 125217.
[31] Wang, L., Kan, A., Yu, W., Melting behavior and heat transfer performance in a modified PCM-filled enclosure with fins under hypergravity conditions, *International Communications in Heat and Mass Transfer*, 138, 2022, 106415.
[32] Sharma, A., Kothari, R., Sahu, S. K., Effect of fin location on constrained melting heat transfer of phase change material in a spherical capsule: A numerical study, *Journal of Energy Storage*, 52, 2022, 104922.
[33] Khedher, N. B., et al., On the application of novel arc-shaped fins in a shell-and-tube type of latent heat storage for energy charge enhancement, *Journal of Energy Storage*, 73, 2023, 108697.
[34] Blázquez, J. L. F., Maestre, I. R., Bahía, Ó. I., Gallero, F. J. G., Hajdukiewicz, M., A new practical approach to design a Phase Change Material-Water longitudinally finned tube heat exchanger, *Applied Thermal Engineering*, 221, 2023, 119834.

[35] Weng, Y.-C., Cho, H.-P., Chang, C.-C., Chen, S.-L., Heat pipe with PCM for electronic cooling, *Applied Energy*, 88, 2011, 1825-1833.
[36] Arumuru, V., Rajput, K., Nandan, R., Rath, P., Das, M., A novel synthetic jet based heat sink with PCM filled cylindrical fins for efficient electronic cooling, *Journal of Energy Storage*, 58, 2023, 106376.
[37] Shakibi, H., Shokri, A., Sobhani, B., Yari, M., Numerical analysis and optimization of a novel photovoltaic thermal solar unit improved by Nano-PCM as an energy storage media and finned collector, *Renewable and Sustainable Energy Reviews*, 179, 2023, 113230.
[38] Bassam, A. M., Sopian, K., Ibrahim, A., Al-Aasam, A. B., Dayer, M., Experimental analysis of photovoltaic thermal collector (PVT) with nano PCM and micro-fins tube counterclockwise twisted tape nanofluid, *Case Studies in Thermal Engineering*, 45, 2023, 102883.
[39] Rahmanian, S., Rahmanian-Koushkaki, H., Omidvar, P., Shahsavar, A., Nanofluid-PCM heat sink for building integrated concentrated photovoltaic with thermal energy storage and recovery capability, *Sustainable Energy Technologies and Assessments*, 46, 2021, 101223.
[40] Zhou, D., Zhao, C.-Y., Tian, Y., Review on thermal energy storage with phase change materials (PCMs) in building applications, *Applied Energy*, 92, 2012, 593-605.
[41] Luo, X., et al., Numerical study on enhanced melting heat transfer of PCM by the combined fractal fins, *Journal of Energy Storage*, 45, 2022, 103780.
[42] Ao, C., Yan, S., Hu, W., Zhao, L., Wu, Y., Heat transfer analysis of a PCM in shell-and-tube thermal energy storage unit with different V-shaped fin structures, *Applied Thermal Engineering*, 216, 2022, 119079.
[43] Palmer, B., Arshad, A., Yang, Y., Wen, C., Energy storage performance improvement of phase change materials-based triplex-tube heat exchanger (TTHX) using liquid–solid interface-informed fin configurations, *Applied Energy*, 333, 2023, 120576.
[44] Zhang, C., Wang, N., Xu, H., Fang, Y., Yang, Q., Talkhoncheh, F. K., Thermal management optimization of the photovoltaic cell by the phase change material combined with metal fins, *Energy*, 263, 2023, 125669.
[45] Ji, C., Qin, Z., Low, Z., Dubey, S., Choo, F. H., Duan, F., Non-uniform heat transfer suppression to enhance PCM melting by angled fins, *Applied Thermal Engineering*, 129, 2018, 269-279.
[46] Khan, Z., Khan, Z. A., Experimental and numerical investigations of nano-additives enhanced paraffin in a shell-and-tube heat exchanger: a comparative study, *Applied Thermal Engineering*, 143, 2018, 777-790.
[47] Alqahtani, T., Mellouli, S., Bamasag, A., Askri, F., Phelan, P. E., Thermal performance analysis of a metal hydride reactor encircled by a phase change material sandwich bed, *International Journal of Hydrogen Energy*, 45, 2020, 23076-23092.
[48] Ma, T., Li, Z., Zhao, J., Photovoltaic panel integrated with phase change materials (PV-PCM): technology overview and materials selection, *Renewable and Sustainable Energy Reviews*, 116, 2019, 109406.
[49] Mahdi, J. M., et al., Simultaneous and consecutive charging and discharging of a PCM-based domestic air heater with metal foam, *Applied Thermal Engineering*, 197, 2021, 117408.
[50] Al-Abidi, A. A., Mat, S., Sopian, K., Sulaiman, M., Mohammad, A. T., Numerical study of PCM solidification in a triplex tube heat exchanger with internal and external fins, *International Journal of Heat and Mass Transfer*, 61, 2013, 684-695.
[51] Zhu, F., Zhang, C., Gong, X., Numerical analysis and comparison of the thermal performance enhancement methods for metal foam/phase change material composite, *Applied Thermal Engineering*, 109, 2016, 373-383.
[52] Liu, Z., Yao, Y., Wu, H., Numerical modeling for solid–liquid phase change phenomena in porous media: Shell-and-tube type latent heat thermal energy storage, *Applied Energy*, 112, 2013, 1222-1232.
[53] Mahdi, M. S., Mahood, H. B., Campbell, A. N., Khadom, A. A., Natural convection improvement of PCM melting in partition latent heat energy storage: Numerical study with experimental validation, *International Communications in Heat and Mass Transfer*, 126, 2021, 105463.
[54] Lv, S., Yang, J., Ren, J., Zhang, B., Lai, Y., Chang, Z., Research and numerical analysis on performance optimization of photovoltaic-thermoelectric system incorporated with phase change materials, *Energy*, 263, 2023, 125850.
[55] Agresti, F., et al., Nano-encapsulated PCM emulsions prepared by a solvent-assisted method for solar applications, *Solar Energy Materials and Solar Cells*, 194, 2019, 268-275.
[56] Kamkari, B., Shokouhmand, H., Bruno, F., Experimental investigation of the effect of inclination angle on convection-driven melting of phase change material in a rectangular enclosure, *International Journal of Heat and Mass Transfer*, 72, 2014, 186-200.

## ORCID iD

Atef Chibani https://orcid.org/0000-0002-5861-7498
Tawfiq Chekifi https://orcid.org/0000-0002-6914-047X
Moustafa Boukraa https://orcid.org/0000-0001-6184-669X



**How to cite this article:** Chibani A., Chekifi T., Boukraa M. Thermal Storage Improvement through the Melting Process of PCMs in Triplex Tube Heat Exchangers with Different Fin Materials, *J. Appl. Comput. Mech.*, 12(1), 2026, 289-301. https://doi.org/10.22055/jacm.2025.48184.5040